Renormalization Group Flow in Lattice QED and Four Fermi Coupling

Masahiro IMACHI

and

Hiroshi YONEYAMA†)

Department of Physics, Kyushu University, Fukuoka 812, Japan

and

Department of Physics, Saga University, Saga 840, Japan†)

ABSTRACT

Renormalization group flow of the $U(1)$ lattice gauge theory with staggered fermions is studied by the Migdal-Kadanoff renormalization group method. The phase structure is extensively investigated. It is shown that an induced four fermi coupling term becomes relevant in the strong gauge coupling region while it becomes irrelevant in the weak gauge coupling one. The chiral order parameter and the anomalous dimension of the fermion mass operator are calculated.

The Migdal-Kadanoff renormalization group (MKRG) method[1,2] is an approximate but suitable tool to get into an essential feature of the lattice gauge models.[3-8] Such a method may provide us with an important information of the dynamics with the strong four fermi coupling, and is complementary to Monte Carlo calculations which are currently providing interesting results.[9-13] One of the authors (M.I.) has recently studied the theory by incorporating the fermion self-energy to the recursion equation, and found that the four fermi interaction is in fact induced from the original QED in the strong gauge coupling region.[14] In the present paper we make an extensive study of its RG flow and the phase structure.

The main results are as follows. The bare parameter space is divided into two phases, one being the phase where the four fermi coupling is relevant and another where it is irrelevant. Within the former phase, there is a distinction with respect to RG flow between the strong and the weak gauge coupling regions. The chiral order parameter shows a transition separating the two phases. The anomalous dimension γ_m of the fermion mass operator is also calculated by the UT(Unique Trajectory[15]) method[5] in the chiral symmetry unbro-

ken phase. It is found that γ_m is large at the critical line and monotonically decreases as one goes off from the critical line, i.e., γ_m decreases monotonically as the gauge coupling and/or the four fermi coupling C_0 become weak.

Migdal-Kadanoff renormalization group transformation

The recursion equations for the MKRG transformation for $U(1)$ LGT with staggered fermions[16,17] are presented .[14] In general, RG transformations induce couplings which are not in the original bare theory. It is then convenient to write here the most general form of action in the MKRG framework. The lattice action of $U(1)$ gauge group with staggered fermions ψ and $\bar{\psi}$ is given by

$$\begin{aligned} S =& S_g + S_f, \\ S_g =& -2\sum_{plaq}\sum_{q=1}^{\infty}(1-\mathrm{Re}\chi_q(\theta))\beta_q, \\ S_f =& A_0\sum_{n,\mu}\eta_\mu(n)(\varepsilon_+\bar{\psi}(n)U_\mu(n)\psi(n+\mu)+\varepsilon_-\bar{\psi}(n+\mu)U_\mu^\dagger(n)\psi(n)) \\ & - B_0\sum_n\bar{\psi}(n)\psi(n) \\ & - C_0\sum_{n,\mu}\bar{\psi}(n)U_\mu(n)\psi(n+\mu)\ \bar{\psi}(n+\mu)U_\mu^\dagger(n)\psi(n), \end{aligned} \tag{1}$$

where χ_q in S_g denotes the q-irreducible character of a plaquette variable ; $\chi_q(\theta) = \mathrm{Tr}U_q = e^{iq\theta}$ (q =integer, $0 \le \theta \le 2\pi$), and β_q is corresponding bare inverse gauge coupling. The fermionic action S_f contains three bare parameters A_0, B_0 and C_0 which represent hopping parameter, mass and four fermi coupling in turn. Positive values of C_0 correspond to an attractive force. ε_+ and ε_- are sign factors ($\varepsilon_+ = -1$ and $\varepsilon_- = +1$), and $\eta_\mu(n) = (-1)^{n_1+n_2+\ldots+n_{\mu-1}}$, where n_i is the i-th coordinate of the site n. The following convention for integrating Grassmann variables ψ and $\bar{\psi}$ is employed:

$$\int d\bar{\psi}d\psi\exp(-p\bar{\psi}\psi+\bar{\psi}\xi+\bar{\zeta}\psi) = p\exp(\frac{1}{p}\bar{\zeta}\xi). \tag{2}$$

A RG transformation consists of two procedures, the decimation and the bond-moving, both for the gauge and fermionic degrees of freedom. In each decimation, the gauge degrees of freedom receive fermion loop corrections, while the fermionic ones contain self-energy corrections.

The recursion equation for the gauge field[3] connecting two scales L and λL is given by

$$F(\lambda L,\theta) = \left[\sum_q \tilde{F}_q(L)^{\lambda^2-1}\tilde{Q}_q(L)\chi_q(\theta)\right]^{\lambda^{D-2}} \tag{3}$$

where $\tilde{F}_q$ is coefficient in the character expansion of the plaquette function $F(L,\theta)$ at scale L,

$$F(L,\theta) = \sum_q \tilde{F}_q(L)\chi_q(\theta), \tag{4}$$

where $F(L,\theta)$ is written in terms of the gauge couplings as

$$F(L,\theta) = F(L,0)\exp\{-2\sum_{q=1}^{\infty}(1-\mathrm{Re}\chi_q(\theta))\beta_q(L)\}. \tag{5}$$

While $\tilde{Q}_q$ is the coefficient in the expansion of $Q(L,\theta)$, which represents the contribution from the innermost plaquette in Fig.1 receiving the fermion loop correction with N_f flavors (vacuum polarization). A RG transformation is thus completed by the bond-moving as is represented by the exponent λ^{D-2} in (3), which is the contribution from the $D-2$ directions perpendicular to the plane on which the plaquette in question is sitting.

The l.h.s. of (3) is also represented by the renormalized couplings $\{\beta_q(\lambda L)\}$ at scale λL in the same manner as (5)

$$F(\lambda L,\theta) = F(\lambda L,0)\exp\{-2\sum_{q=1}^{\infty}(1-\mathrm{Re}\chi_q(\theta))\beta_q(\lambda L)\}. \tag{6}$$

Therefore, by solving (3) and (6) one obtains the recursion equation for the gauge coupling $\{\beta_q(L)\} \to \{\beta_q(\lambda L)\}$.

Through fermion decimation(Fig.2(a))[14] we obtain fermion parameters $A(\lambda L)$, $B(\lambda L)$ and $C(\lambda L)$ at scale λL from those at L. If we take into account fermion self-energy correction(Fig.2(b)), we have

$$\begin{aligned} A_G(\lambda L) &= A(\lambda L)\left(\frac{\tilde{F}_1}{\tilde{F}_0}\right)^{\lambda}, \\ B_G(\lambda L) &= B(\lambda L), \\ C_G(\lambda L) &= C(\lambda L) - \{1-\left(\frac{\tilde{F}_1}{\tilde{F}_0}\right)^{2\lambda}\}A(\lambda L)\varepsilon_+\varepsilon_-. \end{aligned} \tag{7}$$

The factor $\tilde{F}_1/\tilde{F}_0$ is $\sim\beta$ at strong coupling regions ($\beta \ll 1$) and $\sim(1-1/\beta)$ at weak coupling regions($\beta \gg 1$). Then C_G receives large (small) effect from fermion self energy correction in strong (weak) gauge coupling regions. It may be convenient to define normalized parameters M and G rather than using A, B and C. They are defined by

$$M = B_G/A_G, G = C_G/A_G^2.$$

Renormalization group flow and phase structure[18]

We are now ready to calculate RG flow. Throughout this paper the scale factor λ and the number of staggered fermion N_f are taken to be three and unity, respectively. All the calculations in this section are made for a sufficiently small fixed value of B_0 (=0.05). Its extrapolation to B_0=0 will be discussed in the following section.

Flow of the renormalization group transformations runs in the infinite dimensional parameter space, ($\{ \beta_q \quad ; q = 1 \sim \infty \}$, M, G). It may then be convenient to project it to various subspaces. In what follows we, in turn, see the one projected to the subspaces of pure gauge (β_1, β_2), gauge and fermion (β_1, G) and pure fermion (G, M).

Flow diagram of gauge coupling β_q is shown in Fig.3. We observe critical point β_{1c} at $2.3 < \beta_{1c} < 2.4$. For $\beta_1 > \beta_{1c}$, trajectories flow to weaker coupling regions, which represents "screening" due to vacuum polarization. For $\beta_1 < \beta_{1c}$, trajectories flow to IR fixed point $\beta_q = 0$ (q = all).

As to the projection onto the subspace, (β_1, G), the RG flow moves as shown in Fig.4. For each trajectory in the figure, starting point corresponds to the bare theory with certain (β_1, C_0). One clearly sees that the two dimensional subspace (β_1, C_0) is divided into two phases in view of the manner of the movement of the G. For small β_1 and all allowed C_0 values, trajectories move up to large G region very quickly. This feature is seen up to the critical point β_{1c}. In the weak gauge coupling region beyond β_{1c}, trajectories move up first but eventually go down to small G for small C_0 values, while for large C_0 values the trajectories move up quickly to the large G region. Namely, in between strong and weak four fermi coupling regions, a critical line runs (see Fig.7).

Keeping the above feature in mind, let us now see the behavior of the trajectories in the fermionic parameter subspace (M, G); For small $\beta_1 (< \beta_{1c})$;

(1) In the very strong coupling region $\beta_1 (\lesssim 1.0)$, a range of bare theories in different β_1 and C_0 values moves on to a scaling trajectory as seen in Fig.5. The functional form of the trajectory reads $G \propto M^2$ for large M and G values.

(2) As β_1 increases beyond 1.0, the flow starts to deviate from such a trajectory, and the slope of the trajectory becomes smaller in the log$G$-log$M$ plot.

For large $\beta_1 (> \beta_{1c})$, the behavior is quite different from the one for small β_1;

(1) For large bare C_0 values, the trajectories move up as shown in Fig.6.

(2) Whereas for small C_0 values, flows move down and converge to a single trajectory, which moves eventually toward $G = 0$.

(3) In between there exists a critical point C_c, at which trajectory moves flat.

(4) The locations of both the critical C_0 value and the convergent trajectory depend on chosen β_1 value. As β_1 increases, the value of C_c monotonically increases as seen

in Fig.7. Such a critical line (actually critical surface in the full parameter space) separates the parameter space into chiral symmetry unbroken(weak four fermi side) and broken(strong four fermi side) phases. Similar critical line is found also in the analysis of Schwinger-Dyson equation of quenched QED.[19]

(5) On the other hand, the value of G of the convergent trajectory at sufficiently large M decreases, as the bare β_1 increases.

In Fig.7 the two phases are labeled by I (chiral symmetry broken) and II (unbroken). Within the chiral symmetry broken phase I , we found a distinct behavior between strong and weak bare gauge couplings. Trajectories for large bare β_1 values move very slowly toward larger β_1 value, while those for small β_1 converge rapidly to the fixed point at $\beta_q = 0$. This appears to suggest that there is a phase boundary between the two regions. We then distinguish the weaker gauge coupling side from the stronger one by naming it the domain III, as indicated in Fig.7. II and III are then connected to the chiral symmetry unbroken and broken phases, respectively , in the Nambu-Jona-Lasinio model.[20]

Chiral order parameter $< -\bar{\psi}\psi >$ is calculated from the partition function Z by

$$\langle\bar{\psi}\psi\rangle_{B_0} = \frac{-1}{N_{site}}\left[\frac{\partial Z}{\partial B_0}/Z\right]_{B_0}, \tag{8}$$

and by taking linear extrapolation to $B_0 = 0$. N_{site} denotes the total site number, λ^{tD}, with t and D being the number of RG iterations and the space time dimension(=4 in our case), respectively. The result is shown in Fig.8. We observe that $< -\bar{\psi}\psi >$ at strong gauge couplings is much larger than that at weak ones. In the weak gauge coupling region, however, $< -\bar{\psi}\psi >$ is not exactly zero. Subtracting the value ($\approx 5 \times 10^{-5}$) at large β_1, therefore, it can be fitted by an essential singularity form $\alpha\exp(-\gamma/\sqrt{\beta_c - \beta_1})$. The result is insensitive to the assumed value of β_c. For example, a case for β_c=2.3 is shown in the figure.

Anomalous dimension

We will discuss the anomalous dimension of $\bar{\psi}\psi$. Fig.9 shows RG flow for various small values of bare mass B_0 in the symmetric phase (or domain II). One sees that all bare theories (for $C_0 = 0$) with these different values of B_0 converge to single trajectory. Therefore the unique trajectory method applies in order to get the anomalous dimension of $\bar{\psi}\psi$. That is, one sets up a gate on the trajectory , and then count the number of steps t_G of RG transformations necessary to reach the gate from various bare points. The scale at the gate ξ_G and the lattice constant a of a bare point is related by $\log a = -t_G \log\lambda + \log\xi_G$. We found

$$\log B_0 \approx -c(\beta_1)t_G + d(\beta_1), \tag{9}$$

and its slope $c(\beta_1)$ increases as β_1 becomes larger. The $c(\beta_1)$ is calculated to be 0.37, 0.28, 0.19 and 0.14 for β_1=2.5, 3.0, 5.0 and 10.0 in order. This slope gives essentially the anomalous dimension of $\bar{\psi}\psi$ as follows.

The anomalous dimension γ_m is defined by

$$\gamma_m = -\frac{\partial \log m_0(\Lambda)}{\partial \log \Lambda}, \tag{10}$$

where m_0 is a dimensionful bare mass, and Λ denotes an ultraviolet cut-off. In the lattice notation, (10) reads $\gamma_m = \frac{\partial \log B_0(a)}{\partial \log a} - 1$, since $m_0(\Lambda) = B_0(a)/a$ and Λ=$1/a$. γ_m is also represented as

$$\gamma_m = \frac{-1}{\log \lambda}\frac{\partial \log B_0}{\partial t_G} - 1 \tag{11}.$$

For β_1 values in question, (9) leads to

$$\gamma_m \approx c(\beta_1)/\log \lambda - 1. \tag{12}$$

For $\lambda = 3$, γ_m reads $-0.22, -0.41, -0.61$ and -0.71 for β_1=2.5, 3.0, 5.0 and 10.0 in turn. This result seems queer, since it is expected that γ_m is positive and becomes vanishing as β_1 goes to infinity, where the theory becomes free. This is due to the quantitative roughness of the approximation. In the free theory, for example, the mass M ought to change to λM by a scale transformation by λ. However, in the MK framework, or rather generally in approximated RG transformations, M does not transform properly[4] but by λ_{eff} ($\neq \lambda$). Therefore we normalize γ_m in (12) so that $\gamma_m = 0$ is correctly reproduced in the weak gauge coupling limit. Namely, we take λ to be λ_{eff} which is fixed at a large β_1. We choose $\beta_1 = 10.0$ (some other choice, say, $\beta_1 = 15.0$ does not make much difference). The estimated value of λ_{eff} is 1.39. This leads to $\gamma_m = 1.64$, 1.0, 0.36 and 0.0 for $\beta_1 = 2.5$, 3.0, 5.0 and 10.0 (see Fig.10).

References

1. A. A. Migdal, Sov. Phys. JETP **42**, 413, 743 (1976).
2. L. P. Kadanoff, Ann. of Phys. **100**, 359 (1976).
3. S. Caracciolo and P. Menotti, Ann. of Phys. **122**, 74 (1979).
4. T. Matsui, Nucl. Phys. **B136**, 277 (1978).
5. M. Imachi, S. Kawabe and H. Yoneyama, Prog. Theor. Phys. **69**, 221, 1005 (1983).
6. M. Imachi and H. Yoneyama, Prog. Theor. Phys. **78**, 623 (1987).
7. K. M. Bitar, S. Gottlieb and C. K. Zachos, Phys. Rev. **D26**, 2853 (1982).
8. K. M. Bitar, S. Gottlieb and C. K. Zachos, Phys. Lett. **121B**, 163 (1983).
9. J. B. Kogut, E. Dagotto and A. Kocic, Nucl. Phys. **B317**, 253 (1989).
10. J. B. Kogut, E. Dagotto and A. Kocic, Nucl. Phys. **B317**, 271 (1989).

11. S. P. Booth, R.D. Kenway and B. J. Pendleton, Phys. Lett. **228B**, 115 (1989)
12. A. M. Horowitz, Phys. Lett. **219B**, 329 (1989).
13. S.Hands, J.B.Kogut and E.Dagotto , NSF-ITP-89-180.
14. M. Imachi, Prog. Theor. Phys. **81**,1225 (1989).
15. K. G. Wilson and J. Kogut, Phys. Rep. **12C**, 75 (1974).
16. J. Kogut and L. Susskind, Phys. Rev. **D11**, 395 (1975).
17. L. Susskind, Phys. Rev. **D16**, 3031 (1977).
18. M.Imachi and H.Yoneyama, Preprint 1990 Feb., KYUSHU-90-HE-1,SAGA-HE-28.
19. K-I. Kondo, H. Mino and K. Yamawaki, Phys. Rev. **D39**, 2430 (1989).
20. Y. Nambu and G. Jona-Lasinio, Phys. Rev. **122**, 345 (1961).

FIGURE CAPTIONS

Fig. 1. Gauge plaquette decimation. The vacuum polarization is contained. Crosses denote the fermion decimations.

Fig. 2. (a)Link function. (b)Fermion self-energy correction.

Fig. 3. Flow diagrams of gauge coupling constants projected onto (β_1, β_2) plane.

Fig. 4. RG flow projected onto β_1-G plane.

Fig. 5. RG flow projected onto M-G plane. Strong gauge coupling case with $\beta_1 = 1.0$ and C_0=0.0(○), 1.0 (□) and 2.0 (△). Intermediately strong gauge coupling case with $\beta_1 = 2.0$ and C_0=0.0(◇), 1.0(+) and 2.0(×).

Fig. 6. RG flow projected onto M-G plane. Weak gauge coupling case with $\beta_1 = 5.0$ and $C_0 = 0.0$(○), 0.4(□), 0.6(△), 0.9(◇) and 1.0(+).

Fig. 7. Phase diagram in β_1-C_0 plane.

Fig. 8. $< -\bar{\psi}\psi >$ vs. β_1. $C_0 = 0.0$. With fermion self energy correction(○) and without it(□). The former is fitted by $\alpha \exp(-\gamma/\sqrt{\beta_{1c} - \beta_1})$ with $\beta_{1c} = 2.3$, $\alpha = 18.14$, and $\gamma = 12.50$(bold line).

Fig. 9. RG flow projected onto log$M$-log$G$ plane for B_0=0.01(○), 0.025(□), 0.05(△) and 0.1(+). β_1 and C_0 is chosen to be 5.0 and 0.0, respectively.

Fig. 10. γ_m vs. β_1 for $C_0 = 0.0$.

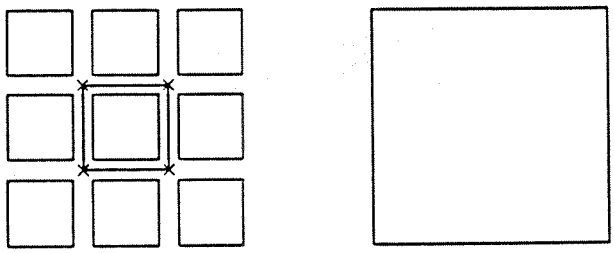

Fig. 1.

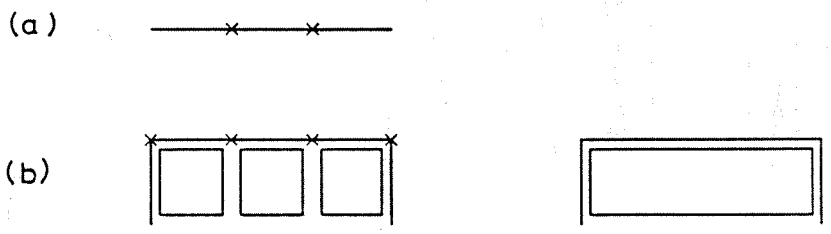

Fig. 2.

Fig. 3

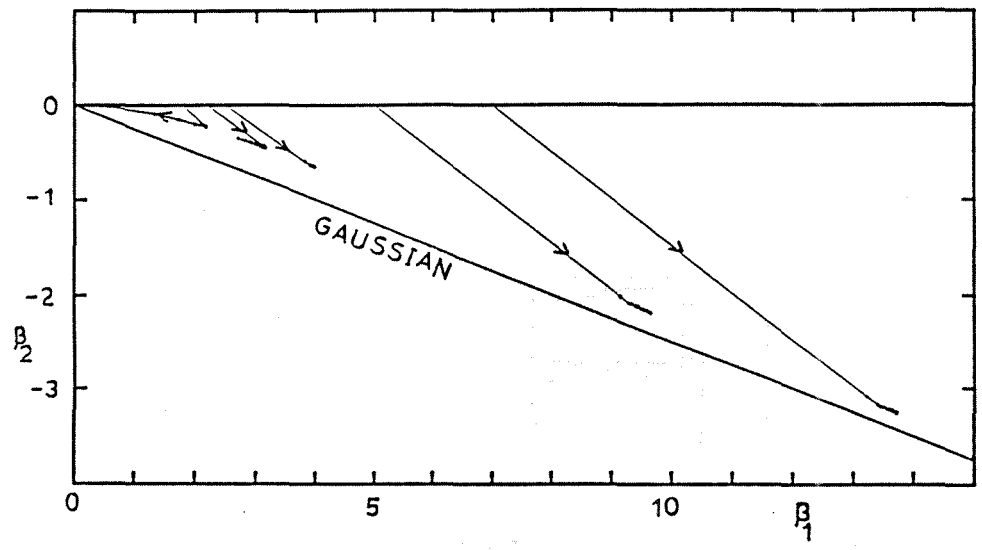

Fig. 4.

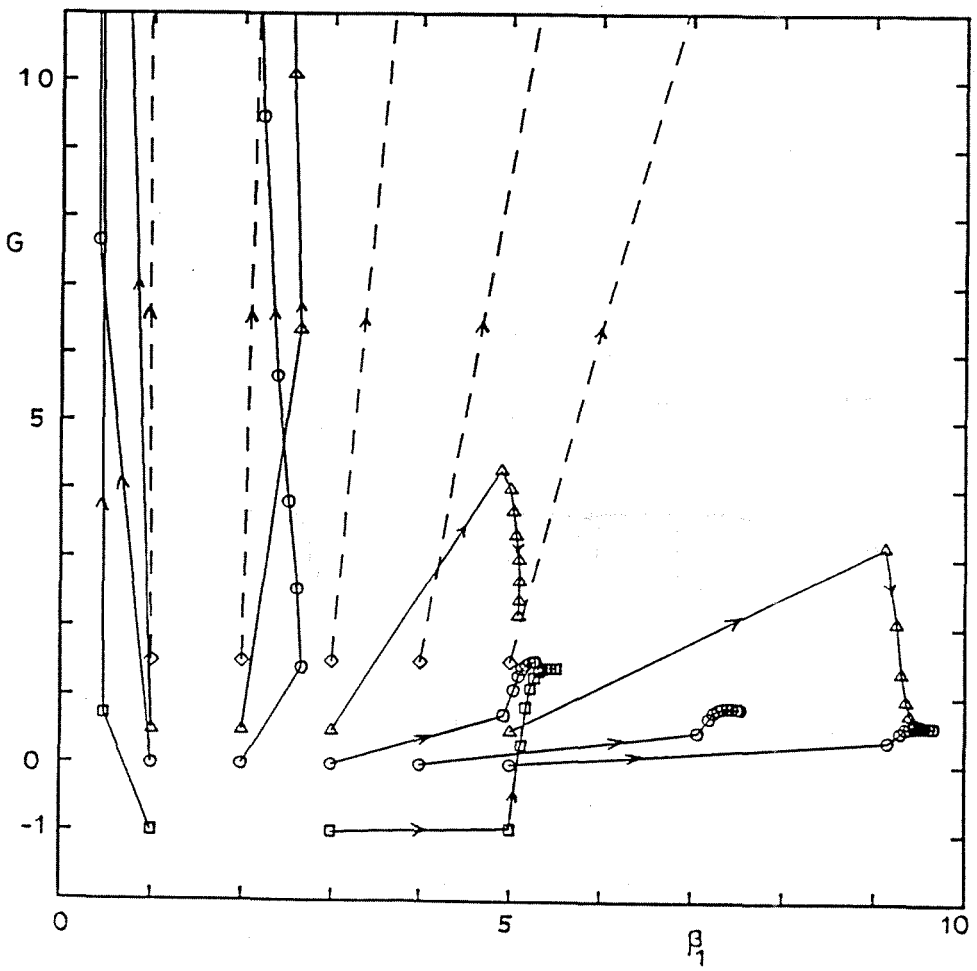

Fig. 5.

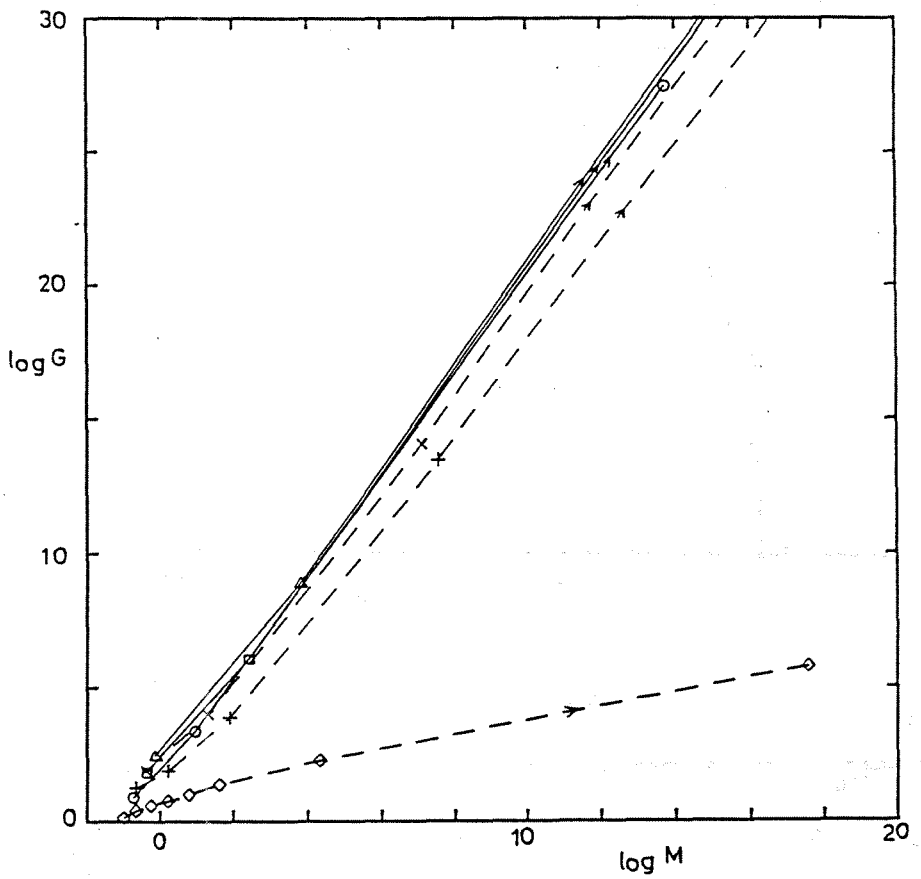

Fig. 6.

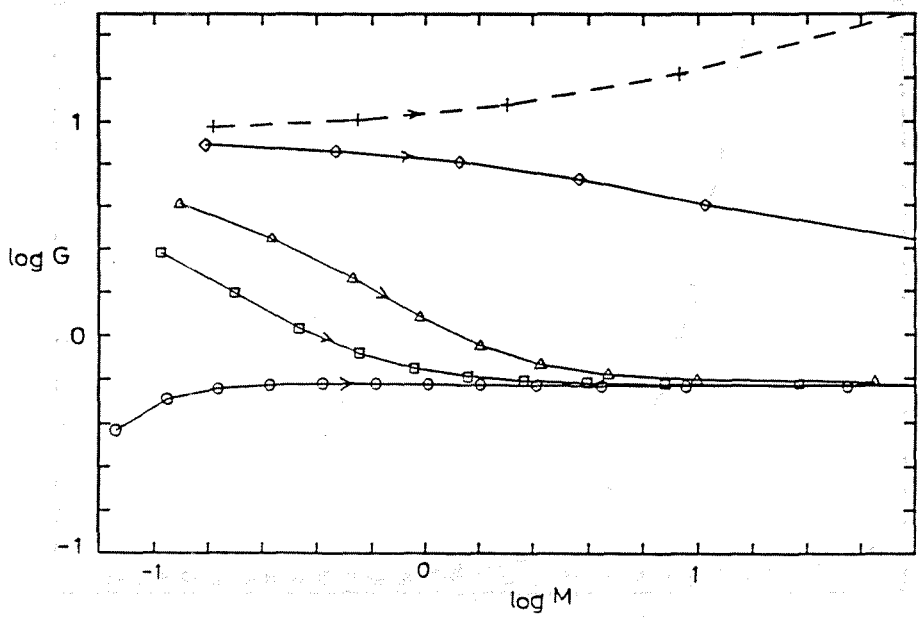

Fig. 7.

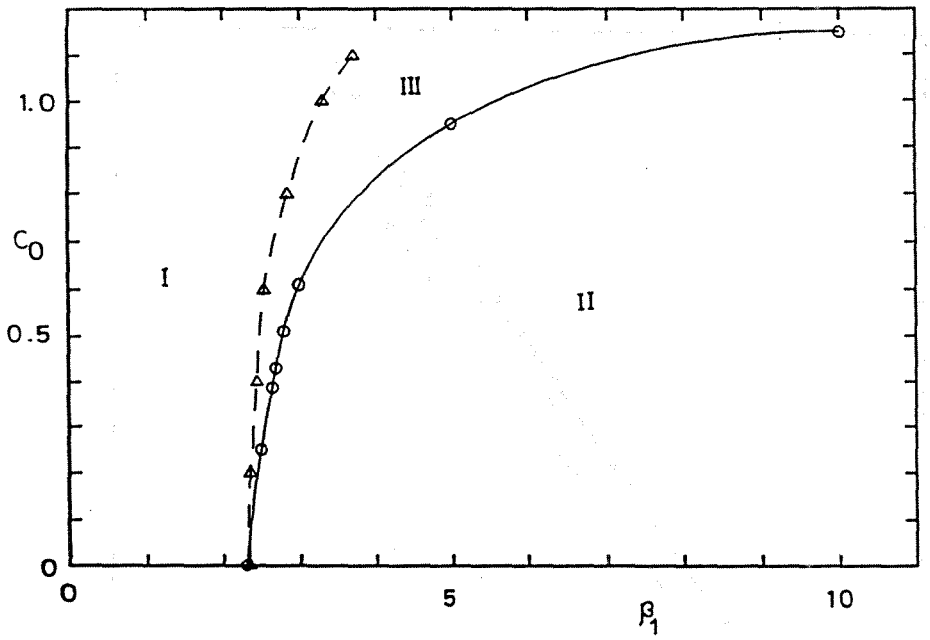
1.0
C_0
0.5
0
I
III
II
0
5
10
β_1

Fig. 8.

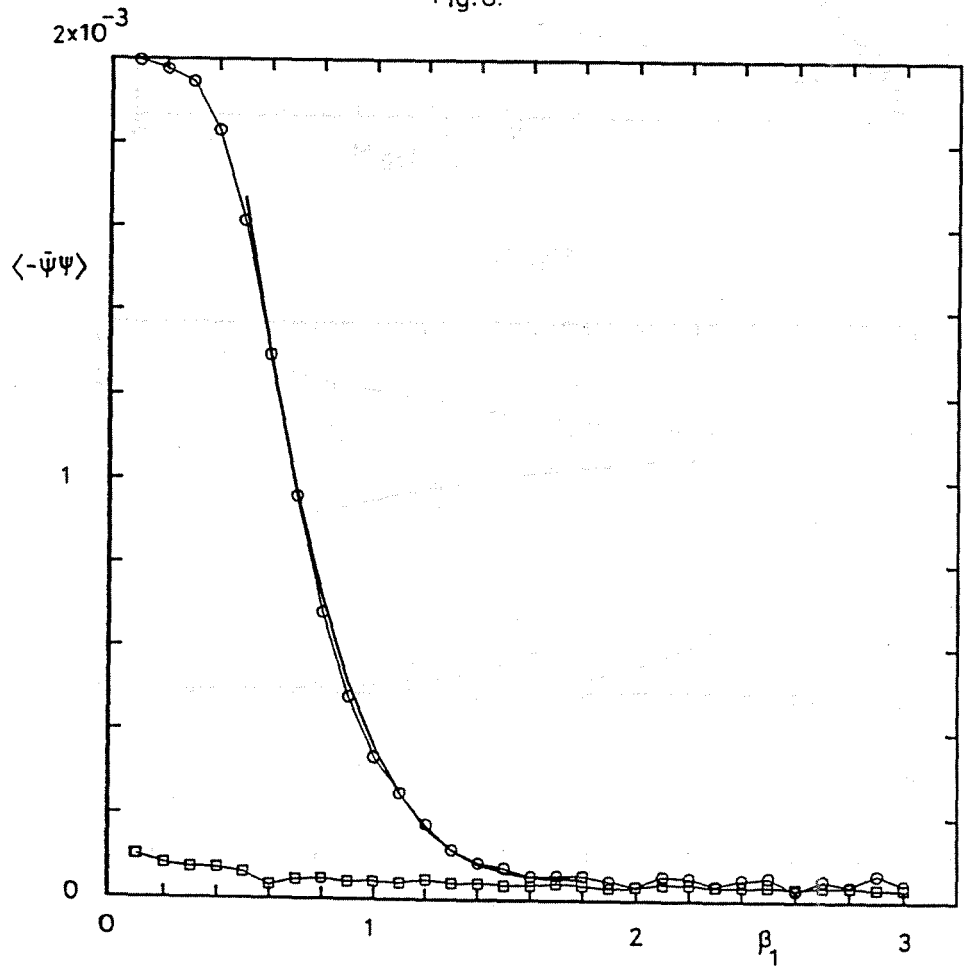
2×10^{-3}
$\langle-\bar{\psi}\psi\rangle$
1
0
0
1
2
3
β_1

Fig. 9 .

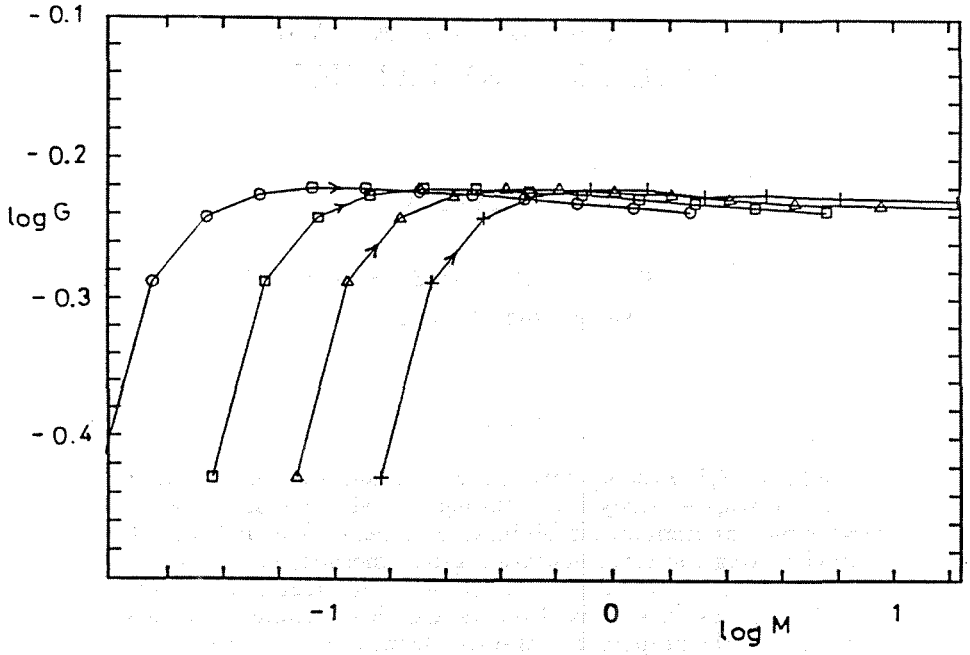

Fig.10.